Backbending and breaking of axial symmetry in the yrast bands of $^{114-130}$Xe isotopes

S. P. Sarswat, Arun Bharti, and S. K. Khosa
P.G. Department of Physics, University of Jammu, Jammu 180004, India
(Received 2 October 1997)

The quadrupole deformation parameter β_2, and energies of yrast states have been calculated in the microscopic frameworks, using the quadrupole-quadrupole-plus-pairing model of a two-body interaction for the even-even isotopic mass chain of xenon isotopes. Results obtained indicate that ground-state deformation systematics are satisfactorily reproduced and there is a breaking of axial symmetry as we move along the yrast states. Besides this, the observed backbending in some of these isotopes is explained in terms of the partial rotational alignment of a pair of neutrons in the $(1h_{11/2})_\nu$ orbit. [S0556-2813(98)00610-4]

PACS number(s): 21.10.Ky, 21.60.Jz, 27.60.+j

I. INTRODUCTION

The study of a chain of xenon isotopes assumed great importance in the past [1–13] because they constitute an important part of a transitional nuclear region in which the nuclear structure makes a smooth transition from a spherical shape to a deformed one. Detailed nuclear structure investigation of these isotopes has been carried out by Saha Sarkar and Sen [14] suggesting the mechanism for the observed $E_{2_1^+}$ systematics. They have calculated the yrast spectra only up to the 2^+ state for all the xenon isotopes, except in the case of ^{122,124}Xe, where the yrast spectra up to 10^+ has been calculated. Since the parameters of their two-body interaction have been fixed by reproducing some of the experimentally observed observable quantities in ^{122,124}Xe, it is quite natural that for these isotopes they are bound to get good agreement with the experimental quantities. Some time back, Kusakari *et al.* [15] reported the existence of high spin states in $^{122-130}$Xe isotopes using in-beam γ-ray spectroscopy. They have also reported the occurrence of backbending in $^{122-130}$Xe nuclei. It is the inquisitiveness to understand the underlying mechanism of backbending that has motivated us to carry out the present work.

In this paper, the results are obtained for the deformation parameter β_2, energy gap parameter for neutrons δ_n, the yrast states, moment of inertia (I) and cranking frequency (ω) in a microscopic framework using pairing-plus-quadrupole-quadrupole effective interaction operating in a valence space spanned by $3s_{1/2}, 2d_{3/2}, 2d_{5/2}, 2f_{7/2}, 1g_{7/2}, 1h_{9/2}$, and $1h_{11/2}$ orbits for protons as well as neutrons. The nucleus ^{100}Sn has been considered as an inert core.

The reason for choosing this model of interaction and the valence space is that we had earlier used the same model of interaction and the valence space for carrying out a detailed study of the complete isotopic mass chain of even-even tellurium isotopes in the mass region $A=120$ [16]. In this paper we have established the applicability of pairing-plus-quadrupole model in this mass region. It may be noted that the interaction parameters used by us in our present calculations of xenon isotopes are exactly the same as used by us in our calculation of tellurium isotopes [16]. In that sense, the present calculation can be thought to involve no free parameters.

The energies of the various angular momentum states have been calculated in both the axially symmetric variation-after-projection (VAP) and nonaxial cranked Hartree-Bogoliubov (CHB) frameworks using the same set of input parameters, interaction and valence space. From the combined data, the yrast spectra is obtained by taking the minimum energy values for each angular momentum state. Results on excitation energy yrast spectra thus obtained indicate that there is a breaking of axial symmetry as we move along the yrast states. The low-lying energy states with spins $J^\pi \leqslant 8^+$ exhibit axial symmetry and higher lying levels with spin $J^\pi \geqslant 8^+$ are seen to be axially asymmetric. This breaking of axial symmetry at 8^+ is found to play an important role in the onset of backbending phenomenon in the xenon isotopes. The results indicate that the cause of backbending in xenon isotopes at higher spins is the partial rotational alignment of a pair of neutrons in the $1h_{1/2}$ neutron orbit near the Fermi surface.

II. CALCULATIONAL DETAILS

The spherical single-particle energies (SPE's) that are employed here are (in MeV): $(2d_{5/2})=0.0$, $(3s_{1/2})=1.4$, $(2d_{3/2})=2.0$, $(1g_{7/2})=4.0$, $(1\ h_{11/2})=6.5$, $(2\ f_{7/2})=12.0$, and $(1h_{9/2})=12.5$. This set of input SPE's for the states $d_{5/2}, s_{1/2}, d_{3/2}, g_{7/2}$, and $h_{11/2}$ is nearly the same as that employed by Vergados and Kuo [17] as well as Federman, Pittel, and Comos [18] except that the energy of $h_{11/2}$ has been increased by about 1.5 MeV. In fact the entire set of spherical single-particle energies is exactly the same as employed by us in our detailed study of even-even tellurium isotopes [16].

The two-body effective interaction that has been employed is of ''pairing-plus-quadrupole-quadrupole $(q-q)$'' type [19]. The pairing part can be written as

$$V_p = -(G/4)\sum_{\alpha\beta} s_\alpha s_\beta a^\dagger_\alpha a^\dagger_{\bar{\alpha}} a_{\bar{\beta}} a_\beta, \qquad (1)$$

TABLE I. Results of VAP and CHB calculations for $^{114-130}$Xe isotopes. Here $\langle Q_0^2\rangle_\pi(\langle Q_0^2\rangle_\nu)$, $\langle Q_2^2\rangle_\pi(\langle Q_2^2\rangle_\nu)$ gives the contribution of the protons (neutrons) to the components of quadrupole moment operator. The seventh column gives the calculated value of quadrupole deformation parameter β_2. The eighth column gives the value of $\gamma-$ the degree of nonaxiality and the ninth column gives the value of δ_n, the energy gap parameter for neutrons. Numbers quoted in square brackets [ ] are experimental values with errors quoted in parentheses ( ). The quadrupole moments have been calculated in units of b^2, where $b=\sqrt{\hbar/m\omega}$ is the oscillator parameter. (Experimental data taken from [14] and [41].)

Nucleus	J^π	$\langle Q_0^2\rangle_\pi$	$\langle Q_2^2\rangle_\pi$	$\langle Q_0^2\rangle_\nu$	$\langle Q_2^2\rangle_\nu$	β_2	$(\gamma)_{\text{Th.}}$	δ_n
^{114}Xe	0^+	20.00	0.00	29.70	0.00	0.275	0.00	1.356
	2^+	20.99	0.00	37.20	0.00	0.307	0.00	1.253
	4^+	20.99	0.00	37.20	0.00	0.307	0.00	1.253
	6^+	21.93	0.00	43.16	0.00	0.333	0.00	1.262
	8^+	20.99	0.00	37.23	0.00	0.307	0.00	1.253
	10^+	20.87	2.94	37.84	5.55	0.340	$-19.3°$	0.820
	12^+	20.70	2.50	38.05	3.76	0.335	$-15.4°$	0.404
	14^+	21.15	2.08	38.24	1.23	0.331	$-10.3°$	0.332
^{116}Xe	0^+	20.89	0.00	38.57	0.00	0.269	0.00	1.546
	2^+	20.89	0.00	38.57	0.00	0.269	0.00	1.546
	4^+	20.89	0.00	38.57	0.00	0.269	0.00	1.546
	6^+	20.89	0.00	38.57	0.00	0.269	0.00	1.546
	8^+	22.28	0.00	51.06	0.00	0.313	0.00	1.193
	10^+	20.42	2.91	35.80	7.00	0.290	$-21.4°$	0.490
	12^+	20.73	2.90	36.15	5.85	0.287	$-19.9°$	0.300
	14^+	20.72	2.77	36.02	4.95	0.283	$-18.3°$	0.242
^{118}Xe	0^+	21.35	0.00	45.88	0.00	0.255	0.00	1.475
						[0.265(6)]		
	2^+	21.35	0.00	45.88	0.00	0.255	0.00	1.475
	4^+	22.37	0.00	51.95	0.00	0.276	0.00	1.030
	6^+	22.37	0.00	51.95	0.00	0.276	0.00	1.030
	8^+	22.37	0.00	51.95	0.00	0.276	0.00	1.030
	10^+	21.31	2.85	46.70	6.88	0.280	$-18.8°$	0.822
	12^+	21.28	2.79	46.15	6.66	0.278	$-18.4°$	0.822
	14^+	21.27	2.70	45.63	6.28	0.276	$-17.8°$	0.800
^{120}Xe	0^+	21.46	0.00	48.02	0.00	0.231	0.00	1.169
						[0.241(11)]		
	2^+	21.46	0.00	48.02	0.00	0.231	0.00	1.169
	4^+	21.82	0.00	52.98	0.00	0.243	0.00	1.358
	6^+	21.82	0.00	52.98	0.00	0.243	0.00	1.358
	8^+	21.82	0.00	52.98	0.00	0.243	0.00	1.358
	10^+	21.48	2.43	45.70	2.19	0.243	$-12.0°$	1.126
	12^+	21.48	2.38	45.21	2.22	0.243	$-12.0°$	1.170
	14^+	21.50	2.21	44.74	2.13	0.241	$-11.4°$	1.224
^{122}Xe	0^+	22.28	0.00	55.11	0.00	0.224	0.00	1.960
						[0.231(10)]		[1.479]
	2^+	22.28	0.00	55.11	0.00	0.224	0.00	1.960
	4^+	22.28	0.00	55.11	0.00	0.224	0.00	1.960
	6^+	22.28	0.00	55.11	0.00	0.224	0.00	1.960
	8^+	22.28	0.00	55.11	0.00	0.224	0.00	1.960
	10^+	22.28	0.00	55.11	0.00	0.224	0.00	1.960
	12^+	22.27	0.14	52.77	0.01	0.240	$-0.52°$	1.120
	14^+	22.40	-0.02	52.23	-0.10	0.240	0.20°	1.074

TABLE I. (*Continued*).

Nucleus	J^π	$\langle Q_0^2\rangle_\pi$	$\langle Q_2^2\rangle_\pi$	$\langle Q_0^2\rangle_\nu$	$\langle Q_2^2\rangle_\nu$	β_2	$(\gamma)_{\text{Th.}}$	δ_n
	0^+	22.33	0.00	52.64	0.00	0.198	0.00	1.045
						[0.264(8)]		[1.386]
	2^+	22.33	0.00	52.64	0.00	0.198	0.00	1.045
^{124}Xe	4^+	22.33	0.00	52.64	0.00	0.198	0.00	1.045
	6^+	22.33	0.00	52.64	0.00	0.198	0.00	1.045
	8^+	21.99	0.00	51.42	0.00	0.195	0.00	0.921
	10^+	21.19	2.90	45.97	9.21	0.208	$-21.56°$	1.160
	12^+	21.13	2.86	45.19	9.31	0.206	$-22.01°$	1.098
	14^+	21.07	2.81	44.24	9.38	0.205	$-21.96°$	1.060
	0^+	22.23	0.00	48.57	0.00	0.174	0.00	1.200
						[0.1881(30)]		[1.313]
	2^+	22.23	0.00	48.57	0.00	0.174	0.00	1.200
^{126}Xe	4^+	21.82	0.00	44.73	0.00	0.167	0.00	0.971
	6^+	21.82	0.00	44.73	0.00	0.167	0.00	0.971
	8^+	21.82	0.00	44.73	0.00	0.167	0.00	0.971
	10^+	21.82	0.00	44.73	0.00	0.167	0.00	0.971
	12^+	21.49	0.00	42.72	0.00	0.162	0.00	0.950
	14^+	21.49	0.00	42.72	0.00	0.162	0.00	0.950
	0^+	21.77	0.00	42.22	0.00	0.149	0.00	1.175
						[0.1837(49)]		[1.269]
	2^+	21.77	0.00	42.22	0.00	0.149	0.00	1.175
^{128}Xe	4^+	21.77	0.00	42.22	0.00	0.149	0.00	1.175
	6^+	21.77	0.00	42.22	0.00	0.149	0.00	1.175
	8^+	21.24	0.00	40.80	0.00	0.145	0.00	1.090
	10^+	20.86	3.04	41.02	11.87	0.169	$-25.95°$	0.720
	12^+	20.50	3.01	33.92	7.12	0.154	$-22.39°$	0.718
	14^+	20.31	3.00	31.87	7.00	0.150	$-22.72°$	1.000
	0^+	21.18	0.00	35.38	0.00	0.127	0.00	1.484
						[0.169(6)]		[1.513]
	2^+	21.18	0.00	35.38	0.00	0.127	0.00	1.484
^{130}Xe	4^+	21.18	0.00	35.38	0.00	0.127	0.00	1.484
	6^+	21.18	0.00	35.38	0.00	0.127	0.00	1.484
	8^+	21.33	0.00	36.90	0.00	0.129	0.00	1.550
	10^+	20.49	2.96	33.53	5.82	0.140	$-20.69°$	1.546
	12^+	20.38	2.91	32.64	6.02	0.138	$-21.04°$	1.440
	14^+	20.24	2.85	31.48	6.15	0.136	$-21.16°$	1.340

where α denotes the quantum numbers $(nljm)$. The state $\overline{\alpha}$ is same as α but with the sign of m reversed. Here S_α is the phase factor $(-1)^{j-m}$. The q-q part of the two-body interaction is given by

$$V_{qq} = -(\chi/2)\sum_{\alpha\beta\gamma\delta}\sum_{\mu}\langle\alpha|q_\mu^2|\gamma\rangle \times\langle\beta|q^2_{-\mu}|\delta\rangle(-1)^\mu a_\alpha^\dagger a_\beta^\dagger a_\delta a_\gamma, \quad (2)$$

where the operator q_μ^2 is given by

$$q_\mu^2 = (16\pi/5)^{1/2} r^2 Y_\mu^2(\theta,\Phi). \quad (3)$$

The strengths for the like particle neutron-neutron $(n$-$n)$, proton-proton $(p$-$p)$, and neutron-proton components of the quadrupole-quadrupole $(q$-$q)$ interaction were taken as

$$\chi_{nn}(=\chi_{pp}) = -0.0122 \text{ MeV b}^{-4},$$

$$\chi_{np} = -0.0230 \text{ MeV b}^{-4}.$$

Here $b(=\sqrt{\hbar/m\omega})$ is the oscillator parameter. These values for the strengths of the q-q interactions compare favorably with the one suggested by Arima [20] and are very near to the ones employed in an earlier study of deformation systematics in the $A\simeq 100$ region by Khosa *et al.* [21] as well as for even even tellurium isotopes [16]. The strength for the pairing interaction was fixed through the approximate relation $G = 18-21/A$ at $G = -0.20$ MeV.

The calculational details of CHB theory are the same as given by Goodman [22] and details of VAP theory are the same as given by Onishi and Yoshida [23] and Baranger [24].

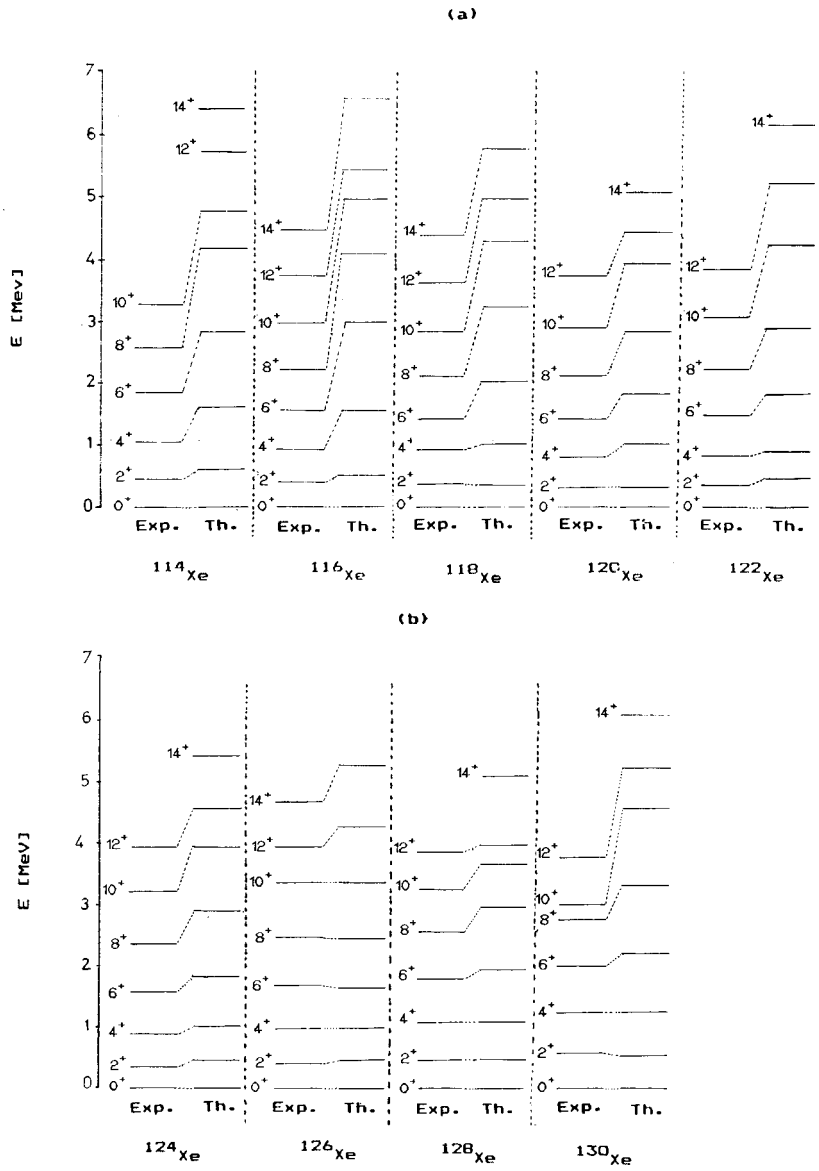

FIG. 1. (a) Comparison of the experimental and calculated yrast spectra in $^{114-122}$Xe. (b). Comparison of the experimental and calculated yrast spectra in $^{124-130}$Xe.

III. RESULTS AND DISCUSSION

A. Results indicating change of symmetry

In Table I, the calculated results on quadrupole moments, quadrupole deformation parameter β_2, asymmetry parameter γ [25] and energy gap parameter δ_n for the set of even-even $^{114-130}$Xe isotopes are presented.

The quantity δ_n for 0^+ state represents the gap between the ground states of even even and odd nuclei and is calculated from the formula $\delta_n = 2\sqrt{(\epsilon_\alpha - \lambda)^2 + \Delta_\alpha^2}$ (Ref. [26]) where λ is the Fermi energy value for neutrons, ϵ_a is the single-particle CHB energy nearest to the Fermi level, and Δ_a is the corresponding energy gap parameter for this single-particle state. From the results presented in Table I, we note that the value of quadrupole deformation parameter β_2 for $^{118-130}$Xe are in reasonable agreement with the experimental values for the 0^+ state. Our values are also comparable to the values calculated by Saha Sarkar and Sen [14].

The results on energy gap parameter δ_n for the 0^+ state are also in reasonable agreement with the observed values for $^{122-130}$Xe isotopes. The satisfactory agreement for β_2 and δ_n clearly shows that our model parameters and the wave functions for the xenon isotopes are fairly reliable.

We now come to the discussion of quadrupole moments and asymmetry parameters. From these results, with the exception of ^{122,126}Xe, all other Xe isotopes are found to exhibit a departure from axial symmetry as we move along the yrast states. The values of $\langle Q_2^2 \rangle_\pi$ and $\langle Q_2^2 \rangle_\nu$ are found to suffer a change from their zero value for lower states to nonzero value for higher angular momentum states. This fact is also shown by a sharp change in the value of asymmetry parameter γ. It may be noted that Xe isotopes with the exception of ^{122,126}Xe have a tendency to be axially symmetric in their low-lying states but they suddenly change their shape so that the nonaxial states appear lower in energy than the axially symmetric state. For example, in $^{114-120,124,128-130}$Xe

isotopes the angular momentum states up to 8^+ are axially symmetric whereas the states higher than $J^\pi > 8^+$ have nonaxial nature. This particular behavior is not exhibited by ^{122,126}Xe. Our calculations show that the axially symmetric intrinsic states and the energy spectra obtained from them through the methods of projection techniques are lower than the corresponding nonaxial projected angular momentum states. Because of this reason, in these two isotopes, the projected angular momentum states producing the yrast spectra in these nuclei arise from such intrinsic states which exhibit a high degree of axiality. As a result of which $\langle Q_2^2 \rangle_{\pi,\nu}$ turn out to be zero and hence $\gamma = 0$ for all the yrast states. It may be noted that Saha Sarkar and Sen's calculations predict an axially symmetric 0^+ state for all even-even xenon isotopes which is also confirmed by our calculations.

We have also presented the excitation energy spectra (Fig. 1) for all the isotopes (experimental values taken from [27–37]). It may be noted that for $^{118-130}$Xe, a satisfactory agreement with the observed values for the states $J^\pi \leqslant 8^+$ is achieved. Thus from these results, we predict the occurrence of breaking of axial symmetry in Xe isotopes as we go to higher spin states.

B. Discussion of results for backbending phenomenon

In Fig. 1, the calculated yrast spectra is compared with the observed (experimental) spectra. It is observed that the systematics of the low-lying states are qualitatively reproduced. The agreement for $J^\pi < 8^+$ for the set of $^{120-130}$Xe isotopes is quite satisfactory.

In Fig. 2, the results of moment of inertia (I) and square of the cranking frequency (ω^2) are plotted for the nuclei ^{114,130}Xe. These quantities have been computed in terms of the yrast energies by using the following expressions [38]:

$$\frac{2I}{\hbar^2} = \frac{4J-2}{E_J - E_{J-2}},$$

and

$$\hbar^2\omega^2 = \frac{[(J^2-J+1)(E_J-E_{J-2})^2]}{(2J-1)^2}.$$

From the experimental backbending plots, backbending is seen to occur at 10^+ in ^{114,128,130}Xe; at 12^+ in ^{122,124,126}Xe; and at 14^+ in ^{118}Xe. It is absent in ^{116,120}Xe isotopes. In the same figure we have plotted the $I-\omega^2$ curves arising from the calculated yrast energies. Our calculated backbending plots also predict the occurrence of backbending at the same spins as is observed experimentally in ^{114,122,124,128}Xe but at different spins in ^{118,126,130}Xe. Besides this, our results also predict occurrence of backbending in ^{116,120}Xe; but experimentally such a backbending is not observed. It, therefore, constitutes a limitation of the present calculation.

In order to understand the mechanism of backbending in xenon isotopes, we have examined the wave function of the higher angular momentum states at which the onset of backbending takes place. The details of these wave functions

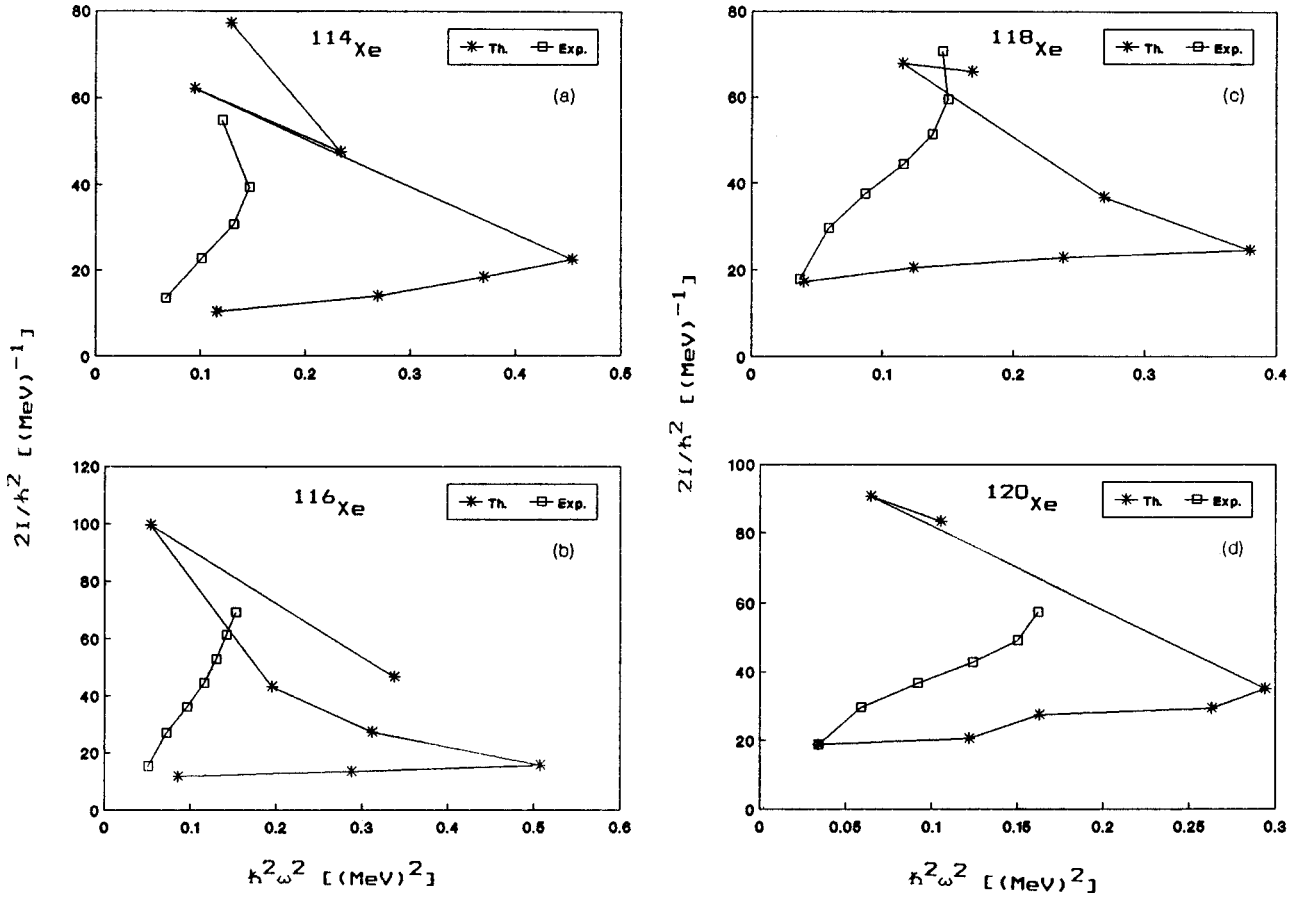

FIG. 2. (a)–(i) Comparison of experimental and calculated $I-\omega^2$ plots for $^{114-130}$Xe.

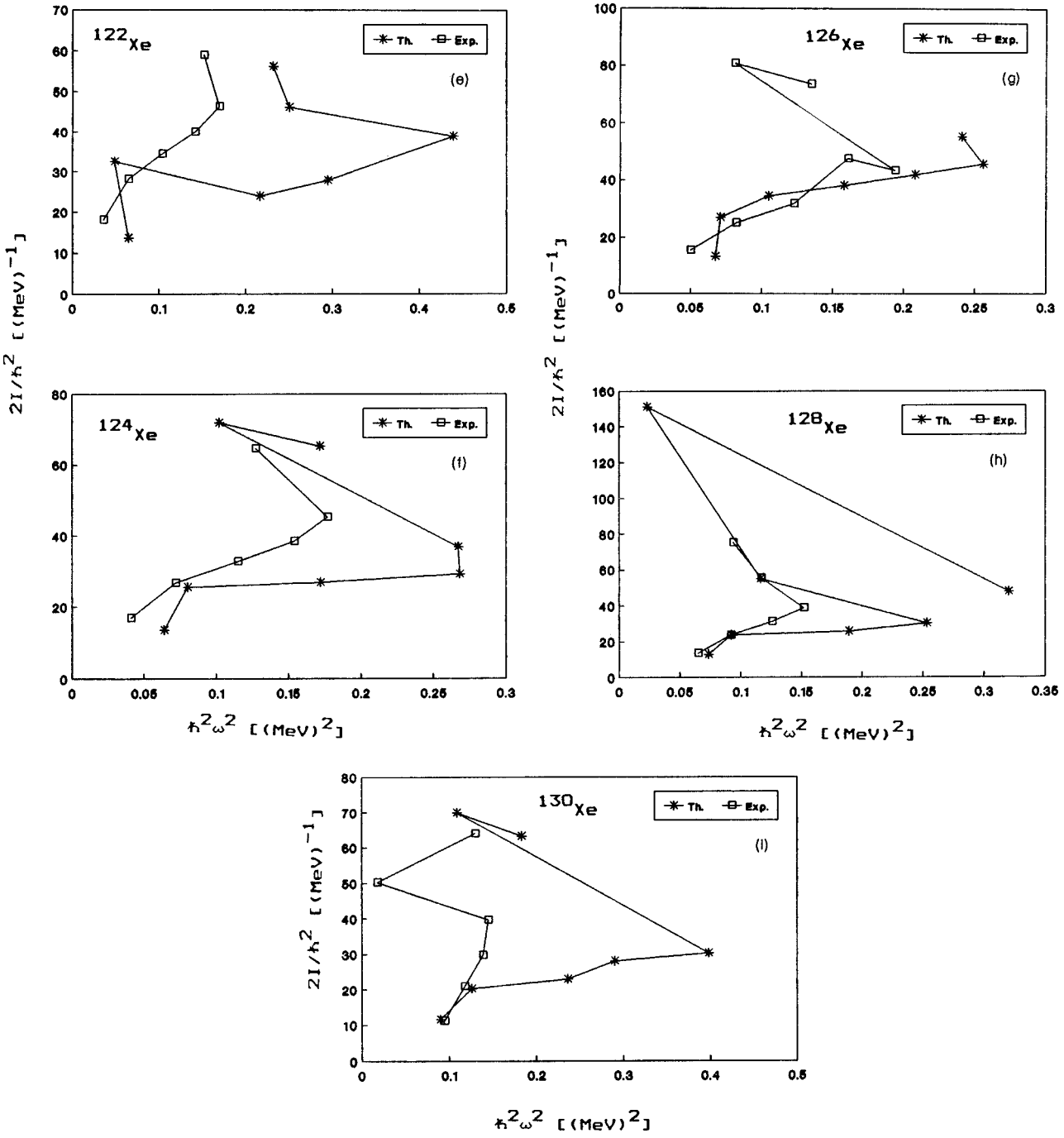

FIG. 2. (*Continued*).

are given in Table II. In these details we have given the values of occupation numbers V_k^2, pairing gap parameters $\Delta_{k,\bar{k}}$ for single-particle CHB orbits, single-particle energies $h_{k,\bar{k}}$ and matrix elements of angular momentum J_k of some single-particle states K which diagonalize the density matrix. It is noted from Table II that the pairing effects decrease considerably for higher angular momentum states. This is indicated by nearly negligible values of the pairing gaps $\Delta_{k,\bar{k}}$ for the higher spin states. It is further interesting to note that the contribution to the the angular momentum $J_k=[\langle J_x\rangle_{k,k}+\langle J_x\rangle_{\bar{k},\bar{k}}]V_k^2$ given in the last column of the table for various K orbits becomes large as we go to the states of angular momentum 14^+. Thus there is a tendency for partial rotational alignment for the pair of neutrons at higher spins in xenon isotopes which can be linked to the occurrence of backbending in these nuclei.

It was shown by Mang [39] that these pairing gap parameters corresponding to the single-particle CHB orbits must decrease for those values of cranking frequency ω at which backbending takes place in a nucleus. These pairing gap parameters of single-particle orbits are different from the values of energy-gap parameters δ_p and δ_n for protons and neutrons.

It has also been suggested by Mottelson and Valatin [40] that the single-particle pairing correlations must considerably decrease at high spins because the Coriolis forces act in opposite directions and tend to decouple the pairing correlations.

TABLE II. Details of $^{114-124,128-130}$Xe wave functions. The occupation probabilities V_k^2, single-particle energies h_{kk}^- and the pairing gaps Δ_{kk}^- are given for five single-particle neutron orbits for the various yrast levels. Here ω denotes the cranking frequency required to obtain various J's. The last column gives the contribution to the angular momentum J' from that of single-particle orbits $J_k=[\langle J_x\rangle_{kk}+\langle J_x\rangle_{KK}^-]V_K^2$ for various K orbits. The nuclide ^{126}Xe has been excluded because of its axial character.

Nucleus	J^π	ω	K	ν_k^2	Δ_{kk}^-(MeV)	h_{kk}^-(MeV)	J_k
^{114}Xe	10^+	0.328	1	1.00	0.0011	−1.39	0.59
			2	1.00	0.0003	0.86	5.66
			3	1.00	0.0010	1.54	1.26
			4	0.00	0.0011	2.16	0.00
			5	0.00	0.0002	2.36	0.00
	12^+	0.400	1	1.00	0.0066	0.47	6.95
			2	0.99	0.0285	1.74	0.97
			3	0.00	0.0192	2.09	0.00
			4	0.00	0.0087	2.32	0.00
			5	0.00	0.1276	2.72	0.00
	14^+	0.446	1	1.00	0.0031	0.15	7.34
			2	0.99	0.0157	1.80	1.31
			3	0.00	0.0102	2.06	0.00
			4	0.00	0.0060	2.28	0.00
			5	0.00	0.0075	2.65	0.00
^{116}Xe	10^+	0.319	1	1.00	0.0026	1.12	4.80
			2	0.99	0.0072	1.46	1.87
			3	0.98	0.0253	2.15	0.44
			4	0.00	0.0066	2.50	0.00
			5	0.00	0.0114	2.92	0.00
^{116}Xe	12^+	0.387	1	1.00	0.0069	0.73	6.07
			2	0.99	0.0257	1.56	1.39
			3	0.98	0.0267	2.12	0.70
			4	0.00	0.0117	2.36	0.00
			5	0.00	0.0190	2.82	0.00
	14^+	0.469	1	1.00	0.0004	0.39	6.80
			2	1.00	0.0018	1.60	1.20
			3	0.99	0.0013	2.05	1.03
			4	0.00	0.0007	2.27	0.00
			5	0.00	0.0010	2.72	0.00
^{118}Xe	10^+	0.297	1	1.00	0.0	0.34	5.66
			2	1.00	0.0	1.42	0.43
			3	1.00	0.0	1.87	1.43
			4	1.00	0.0	2.24	−0.10
			5	0.00	0.0	3.06	0.00
	12^+	0.362	1	1.00	0.0	0.13	6.21
			2	1.00	0.0	1.44	0.56
			3	1.00	0.0	1.82	1.51
			4	1.00	0.0	2.20	0.33
			5	0.00	0.0	3.00	0.00
	14^+	0.430	1	1.00	0.0	−0.11	6.57
			2	1.00	0.0	1.46	0.72
			3	1.00	0.0	1.76	1.62
			4	1.00	0.0	2.14	0.75
			5	0.00	0.0	2.94	0.00
^{120}Xe	10^+	0.297	1	1.00	0.0	0.38	6.31
			2	1.00	0.0	1.69	0.48
			3	1.00	0.0	2.02	0.96
			4	1.00	0.0	2.23	−0.08
			5	1.00	0.0	2.88	−0.28
^{120}Xe	12^+	0.342	1	1.00	0.0	1.99	6.69
			2	1.00	0.0	2.18	0.61
			3	1.00	0.0	2.85	1.14
			4	1.00	0.0	4.04	0.32
			5	1.00	0.0	4.78	−0.12
	14^+	0.400	1	1.00	0.0	−0.06	6.98
			2	1.00	0.0	1.71	0.81
			3	1.00	0.0	1.95	1.28
			4	1.00	0.0	2.12	0.66
			5	1.00	0.0	2.81	0.03
^{122}Xe	12^+	0.438	1	1.00	0.0	−1.05	7.08
			2	1.00	0.0	1.54	1.82
			3	1.00	0.0	1.58	0.07
			4	1.00	0.0	2.24	0.53
			5	1.00	0.0	2.88	−0.21
	14^+	0.495	1	1.00	0.0	−1.28	7.05
			2	1.00	0.0	1.48	2.00
			3	1.00	0.0	1.52	0.59
			4	1.00	0.0	2.22	0.61
			5	1.00	0.0	2.87	−0.09
^{124}Xe	10^+	0.367	1	1.00	0.0	0.17	5.88
			2	1.00	0.0	1.27	0.54
			3	1.00	0.0	1.78	1.75
			4	1.00	0.0	2.21	0.39
			5	1.00	0.0	3.08	0.57
	12^+	0.431	1	1.00	0.0	−0.01	6.22
			2	1.00	0.0	1.26	0.67
			3	1.00	0.0	1.72	1.85
			4	1.00	0.0	2.17	0.74
			5	1.00	0.0	3.02	0.64
^{124}Xe	14^+	0.491	1	1.00	0.0	−0.17	6.41
			2	1.00	0.0	1.26	0.80
			3	1.00	0.0	1.68	1.95
			4	1.00	0.0	2.13	1.04
			5	1.00	0.0	2.96	0.67
^{128}Xe	10^+	0.354	1	1.00	0.0	0.62	4.89
			2	1.00	0.0	1.09	1.06
			3	1.00	0.0	2.06	2.08
			4	1.00	0.0	2.18	0.57
			5	1.00	0.0	3.08	0.70
	12^+	0.377	1	1.00	0.0	1.00	5.08
			2	1.00	0.0	1.43	2.07
			3	1.00	0.0	2.11	0.57
			4	1.00	0.0	2.47	1.56
			5	1.00	0.0	2.87	1.19
	14^+	0.422	1	1.00	0.0	0.97	5.24
			2	1.00	0.0	1.45	2.26
			3	1.00	0.0	2.08	0.70
			4	1.00	0.0	2.50	1.49
			5	0.00	0.0	2.81	1.66
^{130}Xe	10^+	0.369	1	1.00	0.0	5.25	−2.50
			2	1.00	0.0	5.82	−0.18
			3	1.00	0.0	6.42	−2.76
			4	0.00	0.0	7.55	0.00
			5	0.00	0.0	8.54	0.00
	12^+	0.461	1	1.00	0.0	5.24	−2.18
			2	1.00	0.0	5.76	−0.28
			3	1.00	0.0	6.49	−3.07
			4	1.00	0.0	7.53	0.00
			5	1.00	0.0	8.59	0.00
	14^+	0.521	1	1.00	0.0	5.22	−1.78
			2	1.00	0.0	5.68	−0.38
			3	1.00	0.0	6.57	−3.18
			4	1.00	0.0	7.50	0.00
			5	1.00	0.0	8.64	0.00

IV. CONCLUSIONS

Summarizing, it turns out from the results that our model reproduces the deformation and low-level systematics in the even-even isotopic mass chain of Xe isotopes. Besides this, our results also indicate that with the exception of ^{122,126}Xe, all other xenon isotopes are found to exhibit a departure from the axial symmetry, in their yrast spectra at higher spins. The interesting observed backbending phenomenon in the $^{114-130}$Xe isotopes at $J^{\pi} \geqslant 8^{+}$ is explained in terms the partial rotational alignment of a pair of neutrons in the $(h_{11/2})_{\nu}$ orbits.

[1] H. Kusakari, N. Yoshikawa, H. Kawakami, M. Ishihara, Y. Shida, and M. Sakai, Nucl. Phys. **A242**, 13 (1975).
[2] H. Morinaga and N. L. Lark, Nucl. Phys. **67**, 315 (1965).
[3] J. E. Clarkson, R. M. Diamond, F. S. Stephens, and I. Perlman, Nucl. Phys. **A93**, 272 (1967).
[4] I. Brgström, C. J. Herrlander, A. Kerek, and L. Luukko, Nucl. Phys. **A123**, 99 (1969).
[5] J. Genevey-Rivier, A. Charvet, G. Marquier, C. Richard Serre, J. D'Auria, A. Huck, G. Klotz, A. Knipper, and G. Walter, Nucl. Phys. **A238**, 45 (1977).
[6] E. W. Schneider, M. D. Glascock, W. B. Walters, and R. A. Meyer, Phys. Rev. C **19**, 1025 (1979).
[7] B. Singh, R. Iafigliola, K. Sofia, J. E. Crawford, and J. K. P. Lee, Phys. Rev. C **19**, 2409 (1979).
[8] C. Girit, W. D. Hamilton, and E. Michelakakis, J. Phys. G **6**, 1025 (1980).
[9] L. Goettig, Ch. Droste, A. Dygo, T. Morek, J. Srebrny, R. Broda, J. Styczen, J. Hattula, H. Helppi, and M. Jskelinen, Nucl. Phys. **A357**, 109 (1981).
[10] W. Gast, U. Kaup, H. Hanevinkel, R. Reinhardt, K. Schiffer, K. P. Schmittgen, K. O. Zell, J. Wrzesinski, A. Gelberg, and P. V. Brentano, Z. Phys. A **318**, 123 (1984).
[11] R. Reinhardt, A. Dewald, A. Gelberg, W. Lieberz, K. Schiffer, K. P. Schmittgen, K. O. Zell, and P. Von Brentano, Z. Phys. A **329**, 507 (1988).
[12] Dan Jerrestam, S. Elfstrom, W. Klamra, Th. Lindblad, C. G. Linden, V. Barci, H. El-Samman, and J. Gizon, Nucl. Phys. **A481**, 355 (1988).
[13] P. F. Mantica Jr., B. E. Zimmerrman, W. B. Walters, J. Rikovska, and N. J. Stone, Phys. Rev. C **45**, 1586 (1992).
[14] M. Saha Sarkar and S. Sen, Phys. Rev. C **56**, 3140 (1997).
[15] H. Kusakari, K. Kitao, K. Sato, M. Sugawara, and H. Katsuragawa, Nucl. Phys. **A401**, 445 (1983).
[16] Rani Devi and S. K. Khosa, Z. Phys. A **354**, 45 (1996).
[17] J. D. Vergados and T. T. S. Kuo, Phys. Lett. **35B**, 93 (1971).
[18] P. Federman, S. Pittel, and R. Comos, Phys. Lett. **82B**, 9 (1979).
[19] M. Baranger and K. Kumar, Nucl. Phys. **A110**, 490 (1968).
[20] A. Arima, Nucl. Phys. **A354**, 19 (1981).
[21] S. K. Khosa, P. N. Tripathi, and S. K. Sharma, Phys. Lett. **119B**, 257 (1982).
[22] A. L. Goodman, Nucl. Phys. **A230**, 466 (1974).
[23] N. Onishi and S. Yoshida, Nucl. Phys. **80**, 367 (1966).
[24] M. Baranger, Phys. Rev. **130**, 1244 (1963).
[25] A. Bohr, Mat. Fys. Medd. K. Dan. Vidensk. Selsk. **26**, No. 14, 18 (1952).
[26] A. M. Lane, in *Nuclear Theory, Pairing Force Correlations and Collective Motion* (Benjamin, New York, 1964).
[27] S. Raman, J. A. Sheikh, and K. H. Bhatt, Phys. Rev. C **52**, 1380 (1995).
[28] J. Blachot and G. Marguier, Nucl. Data Sheets **74**, 821 (1995).
[29] J. Blachot and G. Marguier, Nucl. Data Sheets **73**, 203 (1994).
[30] K. Kitao, Nucl. Data Sheets **75**, 186 (1995).
[31] A. Hashizume, Y. Tendow, and M. Ohshima, Nucl. Data Sheets **52**, 645 (1987).
[32] T. Tamura, Nucl. Data Sheets **71**, 534 (1994).
[33] T. Tamura, K. Miyano, and S. Ohya, Nucl. Data Sheets **41**, 415 (1984).
[34] T. Tamura, K. Miyano, and S. Ohya, Nucl. Data Sheets **36**, 243 (1982).
[35] K. Kitao, M. Kanbe, and Z. Matumoto, Nucl. Data Sheets **38**, 210 (1983).
[36] Yu. V. Sergeenkov, Nucl. Data Sheets **58**, 785 (1989).
[37] M. Sakai, At. Data Nucl. Data Tables **31**, 399 (1984).
[38] P. N. Tripathi, S. K. Sharma, and S. K. Khosa, Phys. Rev. C **29**, 1951 (1984).
[39] H. J. Mang, in *Proceedings of the International Conference on Nuclear Self Consistent Fields*, edited by G. Ripka and M. Porneuf (North-Holland, Amsterdam, 1975).
[40] B. R. Mottelson and J. G. Valatin, Phys. Rev. Lett. **5**, 511 (1960).
[41] S. Raman, C. H. Malarkey, W. T. Milner, C. W. Nestor, Jr., and P. H. Stelson, At. Data Nucl. Data Tables **36**, 22 (1987).